Visual Abstract

Effect of crack position and size of particle on SIF in SiC particles reinforced Al composite

Aicha Metehri, Madani Kouider, Abdelkader Lousdad
University of Sidi Bel Abbes, Faculty of Technology, Department of Mechanical Engineering, Laboratory of Mechanics Physical of Material (LMPM), 22000, Algeria.
aicha_vie2009@yahoo.fr, koumad10@yahoo.fr, a lousdad@yahoo.com

ABSTRACT. In this paper the effect of reinforcement crack position and loading conditions (in mode I) on the stress intensity factors of the Al/SiC_p metal matrix composite was examined using a finite element method. A simple cubic cell model with square reinforcement shapes was developed to investigate its effect on the mechanical properties of the MMC. The finite element technique was used to calculate the stress intensity factors K_I and K_{II} for crack in the matrix and in particle. The particle and matrix materials were modelled in linear elastic conditions. The obtained results show the important role on the stress intensity factors played by the relative elastic properties of the particle and matrix. The results also show that the loading conditions and inter-distance between two particles with two interfacial cracks has an important effect on the K_I and K_{II} stress intensity factors.

KEYWORDS. Matrix; Reinforced; Composite; Particle; Crack; FIC.

OPEN ACCESS

Citation: Metehri, A., Kouider, M., Lousdad, A., Effect of crack position and size of particle on SIF in SiC particles reinforced Al composite, Frattura ed Integrità Strutturale, 48 (2019) 152-160.

Received: 16.11.2018
Accepted: 28.12.2018
Published: 01.04.2019

INTRODUCTION

Particle-reinforced metal–matrix composites (PRMMCs) are increasingly attracting the attention of automotive and consumer goods industries. Aluminum alloy matrix-reinforced ceramic particles such as SiC, Al_2O_3 are such materials normally used in automobile and aviation.
It is reported that Aluminum reinforced with silicon carbide particles (SiCps) exhibited several advantages in structural applications because of unique properties. This included isotropic mechanical properties, high specific stiffness, high specific modulus, thermal stability and strength as well as high wear resistance. Thus, these composites have found new applications as structural materials in aerospace and automotive industries Zhou (2003) [1].
There are several studies investigating the physical and mechanical properties of metal matrix composites Temel Varol (2013) [2]. Other numerical analyses have been carried out by a number of researchers by considering matrix and reinforcement properties and their respective volume fractions. These analyses approached the problem by considering the unit cell concept of regular array of particles in the matrix. In addition, the shape of the particles was assumed to be either: cylindrical, spherical, rectangular or cubical.

Liu et al (2007) [3] had found that the numerical results with unity aspect ratio were in good agreement with the published experimental data for the effect of reinforcement morphology on the deformation behavior in Al6092/SiCp metal matrix composite.
A series of finite element models have been constructed. Srinivasa et al [4] have shown that the fracture toughness of the composites decreased with an increase in vol% for AlN and decreased in Al_2O_3 particle size. All the composites exhibited R-curve behavior which has been attributed to crack bridging by the intact metal ligaments behind the crack tip. The Young's modulus of the composites increased with the vol% of AlN whereas the thermal diffusivity and coefficient of thermal expansion followed a reverse trend.
The particle size effects on overall deformation behavior of composites come from the particle size effects on deformation and on damage is uniquely determined on the basis of reference length of microstructure such as particle diameter or inter-particle distance. As the fracture strength of brittle materials is higher when the size of sample is smaller, the fracture and debonding of particles in composites is difficult to occur on smaller sized particles this work was the subject of Keiichiro (2010) [5]. The results of Ramazan and al (2015) [6] showed in analysis of a metal matrix composites reinforced with an in-situ high aspect ratio AlB_2 flake that 30 vol% of $A1B_2$/Al composite show a 193% increase in the compressive strength and a 322% increase in compressive yield strength. Results also showed that ductility of composites decreases with adding AlB_2 reinforcements. Bo et al (2015) [7] studied the interaction between a Mode I crack and an inclusion in an infinite medium which was examined under consideration of coupled mechanical and thermal loads under plane strain condition. Finally, the effects of temperature-dependent elastic properties on the inclusion–crack interaction are estimated. It is also found that the shielding or amplifying effect on the crack growth is dependent on the mismatched expansion coefficient if only the variation of temperature is considered.
The results of Omyma et al (2014) [8] showed that the densification and thermal conductivity of the composites decreased with increasing the amount of SiC and increased with increasing SiC particle size. Increasing the amount of SiC leads to higher hardness and consequently improves the compressive strength of Al–SiC composite. Moreover, as the SiC particle size decreases, hardness and compressive strength increase. The use of fine SiC particles has a similar effect on both hardness and compressive strength.
Generally the microscopic failure characteristics of MMCs induced by the coupled loads are in three forms: matrix failure caused by void nucleation and growth; particle breakage and particle/matrix interface de-cohesion.
All these authors did not take into account the presence of a non-emergent crack in a particle composite by FEM whose different positions were highlighted with respect to the particle, on the other hand, the variation of the particle size following the thickness of the composite material has been taken into account in order to see its effect on the value of the stress intensity factor.
The objective of this work is numerically analysis, by FEM. The effect of reinforcement crack position, loading conditions (in mode I) and the size of particle on the stress intensity factors of the Al/SiCp metal matrix composite has been investigated. The first part is to highlight the effect of the crack position (in matrix and in particle) and the size of particle on the stress intensity factors K_I and K_{II}. While the second part presents the investigation of the effect of the interaction between two interfacial cracks (spacing particles) on the stress intensity factors K_I, K_{II} under mode I.

FINITE ELEMENT MODEL

Micromechanical and material model

In general, while in fast fracture state, the SiC particle size has great influence. This is possibly attributed to the different failure mechanisms of crack growth caused by the actions of SiC particle size, shape and distribution [9]. That is why the size of the particle equal to 50μm is selected.
In this study the smallest area of the cross-section and special design was selected as the representative area element. It is assumed that the global behavior of the composite is the same as that of the area element. Fig. 1 shows the micromechanical model used.
A crack of length **a** starting at x=50μm is assumed to be at the interface between the particle and the matrix. The particle and matrix in the model are bonded perfectly with the exception of the crack faces. Frictionless sliding behavior is assumed between the crack faces. A schematic diagram of the randomly arranged particles in the composite material is given in Fig. 1a. The complete cell model is also given in Fig. 1b. Due to symmetry the unit cell model containing only one quarter of particle to reduce the calculation time as well. The length, width and thickness of the particle were 50μm, 50μm and 50μm respectively.

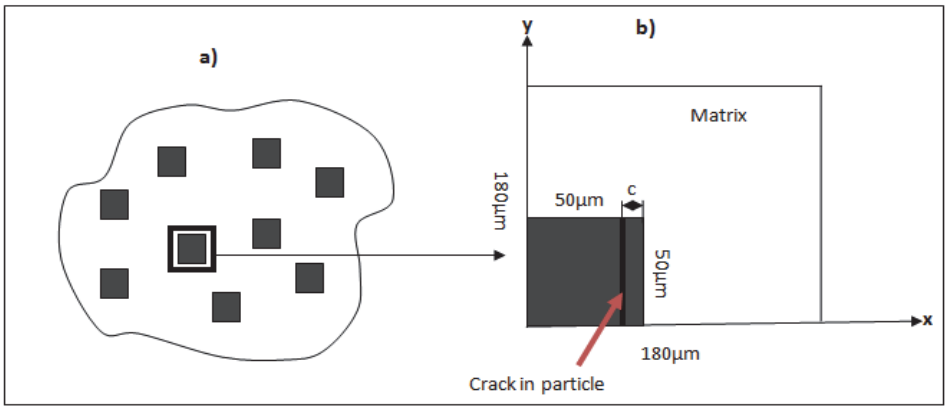

Figure 1: (a) Assumed randomly arranged particles in the overall composite material. (b) The symmetric quarter model in 2D.

In order to develop a three-dimensional finite element for the analysis of the stress intensity factors MMCs, a special design of Al matrix and reinforced particles SiC was proposed as shown in Fig. 2. The produced MMC was subjected to a mechanical load from 50MPa to the 200MPa.
Mechanical characteristics of materials are given in the table below [1]:

Property	Al	SiC
Modulus of elasticity (GPa)	68.3	427
Poisson's ratio	0.33	0.17

Table 1: Mechanicals properties of materials.

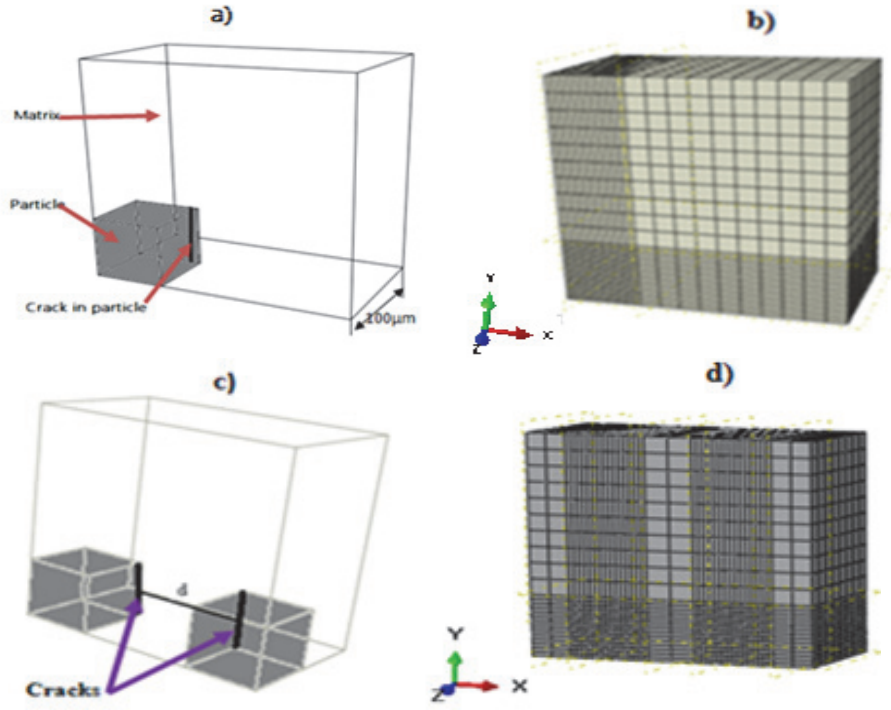

Figure 2: (a) The schematic of assumed MMC model with crack in particle, (b) finite element mesh of model, (c) spacing particles and interaction of two interfacial cracks, (d) finite element mesh of two cubic particles interaction.

FINITE ELEMENT MODEL AND BONDARY CONDITION

Finite element analyzes are performed using FE code Abaqus [10]. Fig. 2 shows the configuration of the crack position in the present model. The symmetry conditions were applied in the finite element solutions as shown in Fig. 3. Hence, It is also assumed that there is no sliding and debonding occurring on the interface of particle–matrix during the loading process.

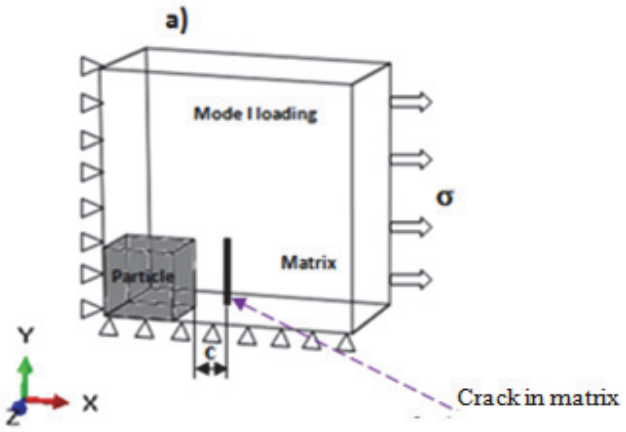

Figure 3: Boundary conditions for mode I loading for crack in matrix.

The distance between the crack in matrix and the interface particle/matrix is c=5µm. The interface crack length is also normalized with 50µm and stress intensity factors are calculated for different y/z ratio of reinforcement is taken as: y/z = 1, y/z= 1.42 and y/z =2.5.

We have set "Y" because at this dimension the particle will have a resistance according to the width of the composite material with particle and therefore less stress concentration which reduces the value of the stress intensity factor at the head of the crack, on the other hand, according to the dimension "Z", the composite material with particle with a weak resistance which pushed us to try to see the variation of dimensioning of the particle following "Z" in order to see the consequences on the ability to reduce stress at the crack.

The precision of numerical computations is strongly related to the quality of the designed mesh surrounding the crack in matrix, or crack in the particle. Thus, a 8-node linear brick (C3D8R) finite element was used for modeling. The elements near the crack are taken as small as possible in order to simulate the stress intensity factors and deformation near the crack more accurately (Fib. 2b). The finite element model is shown in Fig. 3 with 7200 elements. The stress σ is applied along the x-axis for mode I loading (Fig. 3a).

As we know the mesh has a presiding role on the determination of the values of the constraints or the factor of stress intensity. These values are related to the type of elements, numbers of elements and the boundary conditions for our work, we had done a study of convergence of the results or we varied the type of elements and the number of elements. The results do not show a difference except that the calculation time is important considering the existing material and it is for this reason that we took just 1/4 of the structure. For our calculations, the choice was made on the finite element type C3D8R for a linear study.

The number of element type are shown in the Tab. 2 for a 50MPa applied load:

C3D8R	Number of nodes	elements Number	K_I
1- Normal mesh	8729	7200	5.02MPa.mm$^{1/2}$
2- Medium mesh	19286	16848	5.026MPa.mm$^{1/2}$
3- Raffini mesh	38655	34848	5.053MPa.mm$^{1/2}$

Table 2: Number and type of element.

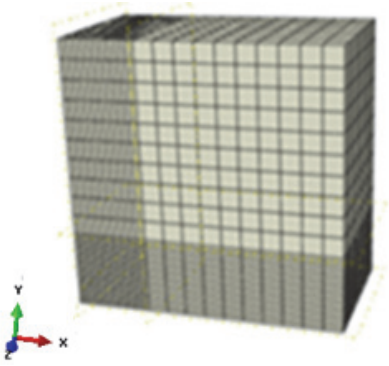

Figure 4: Normal mesh

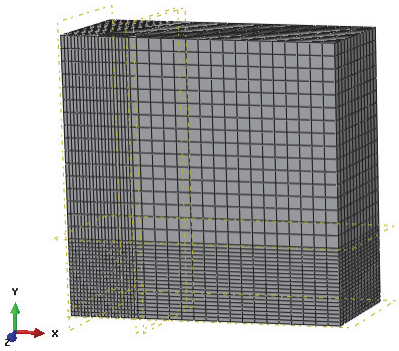

Figure 5: Medium mesh

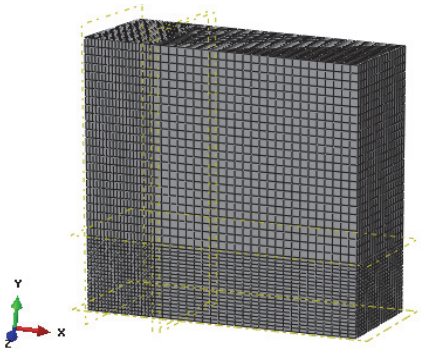

Figure 6: Raffini mesh

RESULTS AND DISCUSSION

Effect of the Crack position on the stress intensity factors

For better illustrating the influence of the crack position on the variation of the stress intensity factors in particle/reinforced metal-matrix composites; a crack length a=50µm (the critical state of a crack). In this section it is assumed that the length, width and thickness of particle are 50µm, 50µm, 50µm respectively. The matrix has the following dimensions: the length 180µm, the width 180µm and the thickness is 100µm.

We had the choice to vary the length and the width of the crack but for our study, we did not want to highlight several parameters at once, so we took the case where the crack has the same size as the particle. Other studies are in progress and which aim to vary the size of the crack and to see the report width of crack, length of the crack on the factor of stress intensity.

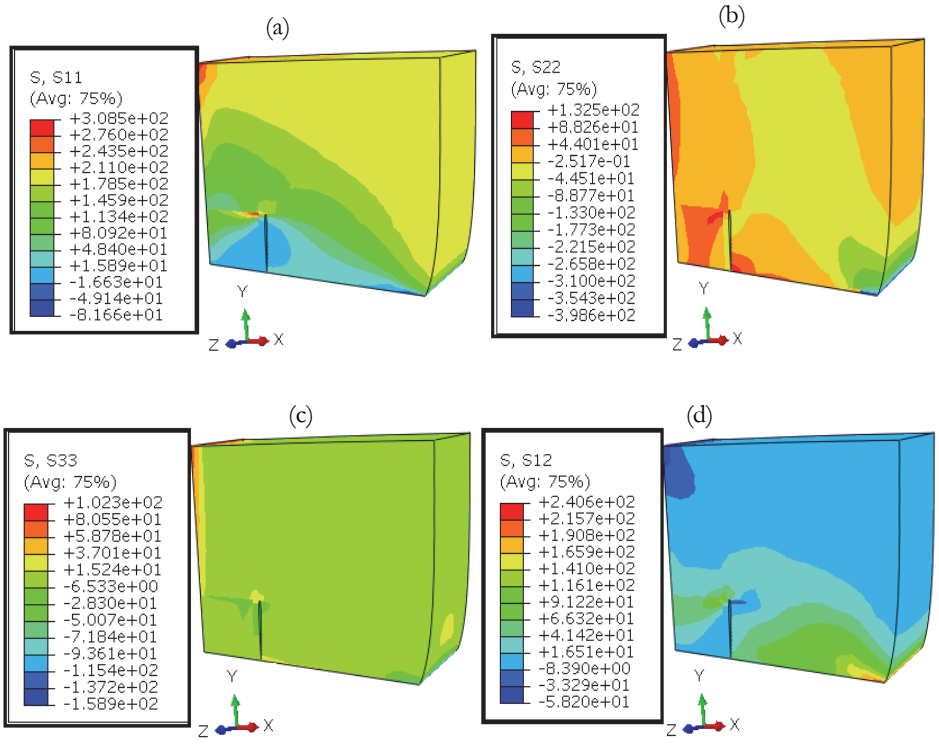

Figure 4: Normal and shear stresses distribution at the crack tip for σ = 200MPa in the matrix (mode I): (a) σ_{xx}, (b) σ_{yy}, (c) σ_{zz}, (d) σ_{xy}.

In the matrix

The evaluation of stress intensity factors, K_I and K_{II} at the crack tip are determined by using the finite element solutions. The existence of a crack in the matrix at a vicinity of the interface particle/matrix with the distance c=5μm and the length a=50μm was studied as shown in Fig. 4 where the normal and shear mechanical stresses distributions at the crack tip are given for σ=200MPa. It is observed that the normal and shear stresses are higher at the crack tip for mode I loading.

Variations of K_I and K_{II} for the crack in the matrix depending on the different ratio of reinforcement and load applied are given in Fig. 5. K_I values for the crack in matrix in the vicinity of the interface particle/matrix (c=5μm) are higher than K_{II} values. The opening mode K_I takes positive values (18 MPa.mm$^{1/2}$) for all applied loads on the cell that exert to open the crack faces. The cause of this is the higher crack tip nodal displacement due to the load.

K_{II} takes a negative value (equal approximately to -1.4 MPa.m m$^{1/2}$) when the y/z ratio is decrease under mode I loading conditions. It is possible to say that loading condition does not have much effect on K_{II} value for the ratio y/z=2.5. The effect of interaction crack– interface is highlighted when the crack length (a=50μm) tends towards the half of the thickness of the cell (e=100μm) and particularly for that containing the crack [11]. Indeed, a tendency of the crack towards the interface leads to a strain field at the crack tip more significant due to the interaction with the interface. The crack position in the matrix leads to the maximum SIF values in mode I when the y/z ratio is decrease. These results indicate that deformation fields in the vicinity of the crack tip are dominated by opening mode K_I value.

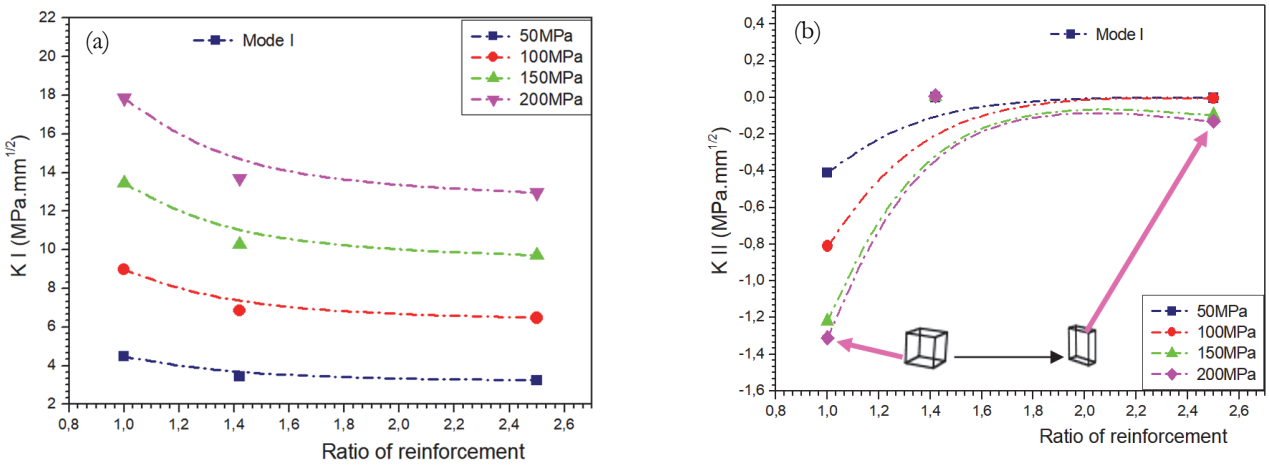

Figure 5: Variation of K_I and K_{II} with different ratio of reinforcement and applied load for the crack in the matrix.

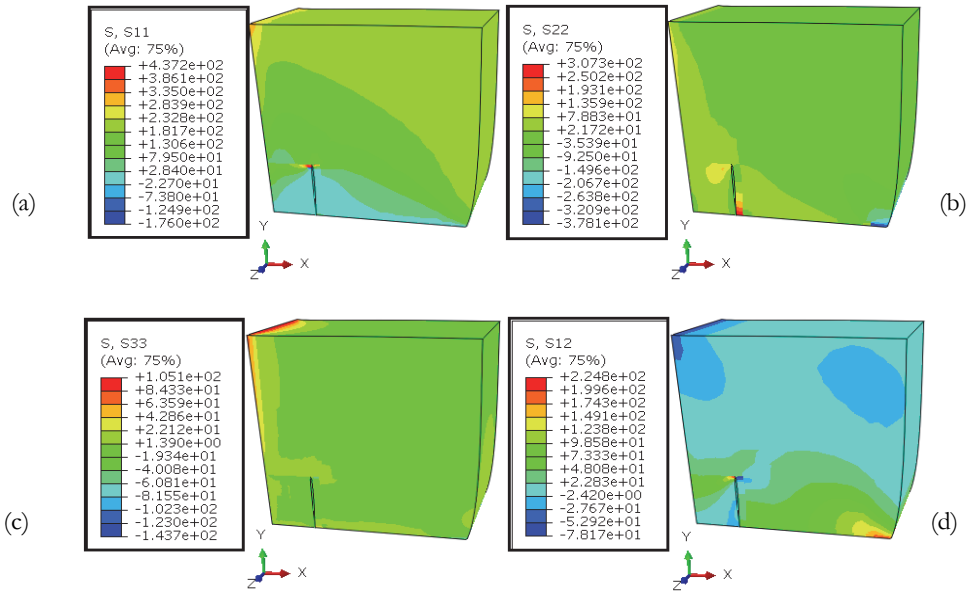

Figure 6: Normal and shear stresses distribution for σ = 200MPa in particle (mode I): (a) σ_{xx}, (b) σ_{yy}, (c) σ_{zz}, (d) σ_{xy}.

In the particle

In this case the presence of a crack (parallel to the interface particle/matrix) in particle is considered and the effect of the different ratio of reinforcement and loading conditions on the energy of crack propagation characterized by the stress intensity factors are taken into account. The crack length is equal to 50µm and the distance between interface and crack in particle is c=5µm. Fig. 6 shows the normal and shear stresses distribution at the crack tip given for σ=200MPa.

Fig. 7 shows the variations of K_I and K_{II} stress intensity factors with the different aspect ratio of reinforcement and applied load under mode I loading. It can be seen that for all applied loads, in general, for the crack length (a=50µm), K_I and absolute K_{II} values increase. Furthermore, one can notice that the opening and the sliding mode of the crack are more intense in the cases of existence of the crack in the particle. It can be also noticed that the existence of a crack in particle facilitates the sliding of the crack. At the same time it facilitates the opening of the crack propagation because the values of K_I and K_{II} in particle are higher than the values of K_I and K_{II} in matrix which is due to the high elastic modulus of the particle. The increase in K_I value is linear depending on the ratio of reinforcement. It is observed that the maximum value of K_I or the maximum absolute value of K_{II} are registered at y/z=1 (K_I 20 MPa.mm$^{1/2}$ for a=50µm) under mode I loading. The level of this stress intensity factors decreases with the increase in the y/z ratio.

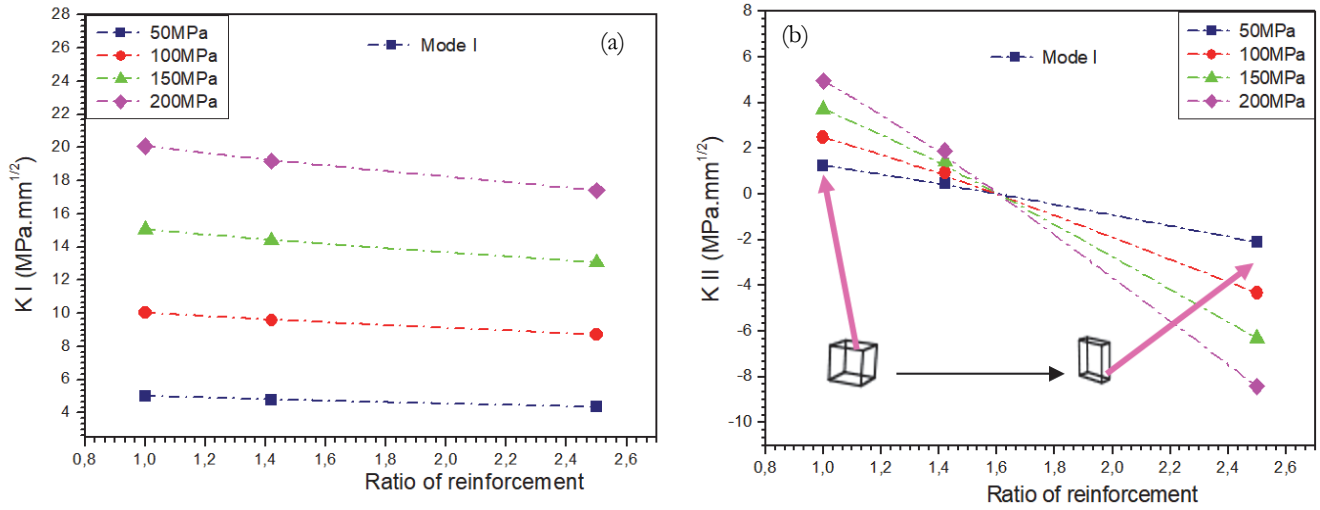

Figure 7: Variation of K_I and K_{II} with ratio of reinforcement and applied load for the crack in the particle.

Inter-distance effect on the SIF

In this part, we study the inter-distance effect of the two interfacial cracks between two cubic particles on the evolution of the stress intensity factors K_I and K_{II} is considered.

The distance 'd' is the interdistance separating the interfacial cracks tips from the first particle and the second particle as presented in Fig. 2c. The displacement of the interfacial cracks of length a=50µm are parallel to the y-axis. The results obtained for the applied loading conditions for σ=150MPa are illustrated in Fig. 8.

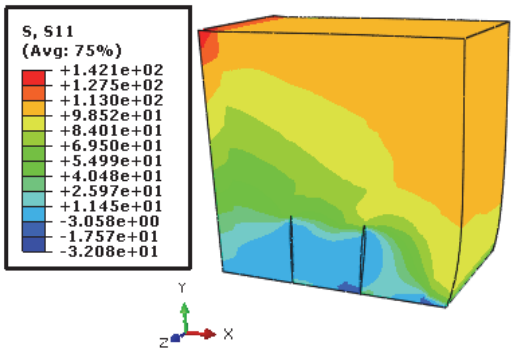

Figure 8: Mechanical stress distribution at the crack tip cases of interfacial crack–crack interaction (two cubic particles interaction for σ = 150MPa).

Fig 9 shows the variations of K_I and K_{II} stress intensity factors according to the distance between two interfacial and parallel cracks for two cubic particles and for different applied loads with thickness of particle fixed at 50µm. It is observed that for d=15µm, both K_I, absolute values K_{II} are more intense than other inter-distances. K_I decreases when'd' increases (Fig. 9a). As we can see that the variation of the SIF K_I is inversely proportional to the distance between two interfacial cracks and stabilizes when the two particles either at the end of the model.
In fact, an almost 5 time decrease in the inter-particle spacing leads to a significant increase in the K_I. The shearing mode K_{II} stress intensity factor (Fig. 9b) seems to be independent to inter-distance '**d**' since these values are very low compared to K_I. Thus, the opening fracture mode is the preponderant one. The latter shows that this failure criterion is closely linked to the spacing particle. This is mainly due to increased tensile stresses. The risk of failure to the composite material is real when the spacing interfacial cracks are very small.

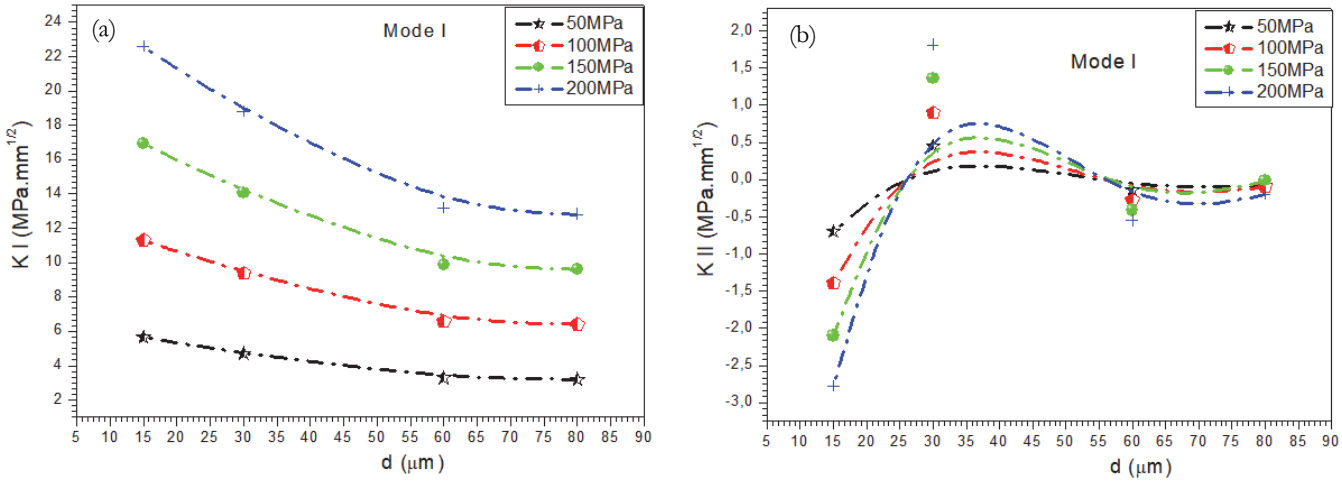

Figure 9: Variation of K_I and K_{II} versus particles spacing (two cubic particles case) and applied load.

CONCLUSION

In this study a finite element model is developed to calculate the stress intensity factors in mode I and mode II (K_I and K_{II}) under mode I loading condition. From the general results of the investigation the following conclusions can be drawn:
For the considered loading conditions (mode I) and for all crack position:

- The higher mechanical load occurring at the crack tip and the deformation fields in the vicinity of the crack tip are dominated by the opening mode.
- For the position of the crack in the matrix the stress intensity factor K_I is high (18 MPa.mm$^{1/2}$), the stress intensity factor K_I decreases if the particle size decreases, by increasing the applied load, the value of the stress intensity factor increase considerably. The difference compared with the other curves (50MPa and 200MPa) is approximately 28% for the ratio y/z =1, and almost 22% for the ration y/z = 2.5 which is almost equal to the 1/4. Also, the value of the stress intensity factor K_{II} increases by decreasing the ratio y/z, the increase in the applied load causes an increase in the K_{II} up to a ratio y/z = 1, once this ratio is exceeded, the effect of the applied load disappears.
- For the position of the crack in particle the risk of propagation by opening effect is very important since the value of K_I is very high (K_I 20 MPa.mm$^{1/2}$). One can conclude that same behavior in this case of the stress intensity factor K_I for the position of the crack in the matrix. The difference lies between 23% and 25% for the two ratios (y/z =1 and y/z=2.5). The absolute value of the stress intensity factor K_{II} increase by decreasing of the size of particle. The increase in the applied load causes an increase in the absolute K_{II} value to the ratios y/z =1 and 2.5; with his sign is changed.
- The particle spacing can affect the stress intensity factors by influencing the interaction between the particles. The SIF increases with a decrease in particle spacing. A 5-time decrease in inter-particle spacing can lead to a 2-time increase in K_I stress intensity factor (SIF equal to 23MPa.mm$^{1/2}$ for σ=200MPa).

REFERENCES

[1] Zhou, Y.C, Long, S.G., Liu, Y.W. (2003). Thermal Failure Mechanism And Failure Threshold Of SiC Particle Reinforced Metal Matrix Composites Induced By Laser Beam, Mechanics of Materials, 35, pp. 1003–1020. DOI: 10.1016/S0167-6636(02)00322-8.

[2] Varol, T., Canakci, A. (2013). Effect of particle size and ratio of B4C reinforcement on properties and morphology of nanocrystalline Al2024-B4C composite powders, Powder Technology 246, pp. 462 –472. DOI: 10.1016/j.powtec.2013.05.048.

[3] Chan, K.C., Tang, C.Y. (2007), Effect Of Reinforcement Morphology On Deformation behavior of particle reinforced metal matrix composites in laser forming, Computational Materials Science, 40, pp. 168–177. DOI: 10.1016/j.commatsci.2006.12.007

[4] Boddapati, S. R., Rodel, J., Jayaram, V. (2007). Crack Growth Resistance (R-curve) Behavior And Thermo-Physical Properties Of Al_2O_3 Particle-Reinforced AlN/Al Matrix Composites, Composites: Part A 38, pp. 1038–1050. DOI: 10.1016/j.compositesa.2006.06.015

[5] Tohgo, K., Itoh, Y., Shimamura, Y. (2010). A Constitutive Model Of Particulate-Reinforced Composites Taking Account Of Particle Size Effects And Damage Evolution, Composites: Part A 41, pp. 313–321. DOI: 10.1016/j.compositesa.2009.10.023.

[6] Ramazan, K, Ömer, S. (2015). Fabrication and properties of in-situ Al/AlB_2 composite reinforced with high aspect ratio borides, Techno press, pp. 777-787. DOI: 10.12989/scs.19.3.777.

[7] Bo, P., Miaolin, F., Jinquan, F. (2015). Study on the crack–inclusion interaction with coupled mechanical and thermal strains, Theoretical and Applied Fracture Mechanics, 75, pp. 39-43. DOI: 10.1016/j.tafmec.2014.10.006.

[8] El-Kady, O., Fathy, A. (2014). Effect of SiC particle size on the physical and mechanical properties of extruded Al matrix nanocomposites, Materials and Design, 54, pp. 348–353. DOI: 10.1016/j.matdes.2013.08.049

[9] Li, W, Liang, H., Chen, J., Zhu, S. Q., Chen, Y. L. (2014). Effect Of SiC Particles On Fatigue Crack Growth Behavior Of SiC Particulate-Reinforced Al-Si Alloy Composites Produced By Spray Forming; Procedia Materials Science 3, pp. 1694 – 1699. DOI: 10.1016/j.mspro.2014.06.273.

[10] ABAQUS/CAE Ver 6.9. (2007). User's Manual. Hibbitt, Karlsson & Sorensen, Inc.

[11] Madani, K., Belhouari, M., Bachir Bouiadjra, B., Serier, B., Benguediab, M. (2007). Crack Deflection At An Interface Of Alumina/Metal Joint: A Numerical Analysis; Computational Materials Science. 38, pp. 625–630. DOI: 10.1016/j.commatsci.2006.04.0060.